DEVELOPMENT OF COMPOSITE ANISOGRID SPACECRAFT ATTACH FITTING

A.F.Razin and V.V.Vasiliev

Central Research Institute for Special Machinery
Khotkovo, Moscow Region 141371, Russia

ABSTRACT

The paper is concerned with a composite spacecraft attach fitting (adapter) which provides the interface between a spacecraft and a commercial launcher. Typical adapter structure is a thin-walled conical shell with the larger diameter about (2-4) m and height (1-2) m loaded with axial compressive forces and bending moments of rather high level and experiencing low frequency vibration.

Because the adapter belongs to the highest stage of the launching system, its weight efficiency is of primary importance and call for modern composites as structural materials. Typical composite adapters are built in the form of stringer stiffened structures, sandwich shells and truss systems.

Anisogrid lattice composite adapter discussed in the paper is characterized with extremely high weight efficiency and relatively low cost. It consists of symmetric system of helical ribs directed along geodesic lines of the conical surface, circumferential ribs and end rings. Adapter is fabricated of carbon-epoxy composites by continuous winding.

In application to a lattice composite adapter, the following problems are discussed

- design for minimum mass,
- finite element analysis,
- manufacturing process,
- testing.

Design, manufacturing and testing of composite lattice adapters are demonstrated for Russian Proton-M adapter. Experience of manufacturing, application and efficiency of this adapter is discussed below.

1. INTRODUCTION

Payload attach fitting (adapter) is a primary structure of a commercial launcher providing the interface between a rocket and a spacecraft. Because the diameters of attach rings of a launcher and of a spacecraft are usually significantly different and the distance between the rings is relatively small, a typical adapter is a conical shell with rather high angle between its meridian and the launcher axis.

Existing adapters are made in the form of stringer stiffened or sandwich aluminum or carbon-epoxy composite shells. Because the adapter is covered with a rocket fairing while launching, its can be also made in the form of a truss or a lattice structure consisting of a system of ribs. In application to spacecraft adapters, truss and lattice composite structures are discussed in Ref. [1-3]. Anisogrid composite lattice structures [4] that have shown high performance and weight efficiency for interstage sections [4] are discussed below in application to Proton-M commercial rocket adapter [5].

2. DESIGN AND ANALYSIS

A typical anisogrid lattice composite payload adapter is shown in Figure 1, whereas its geometry is presented in Figure 2.

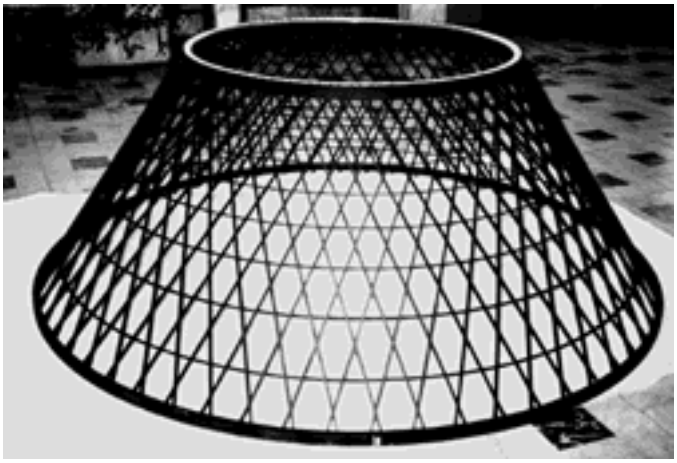

Figure 1. Anisogrid composite payload adapter

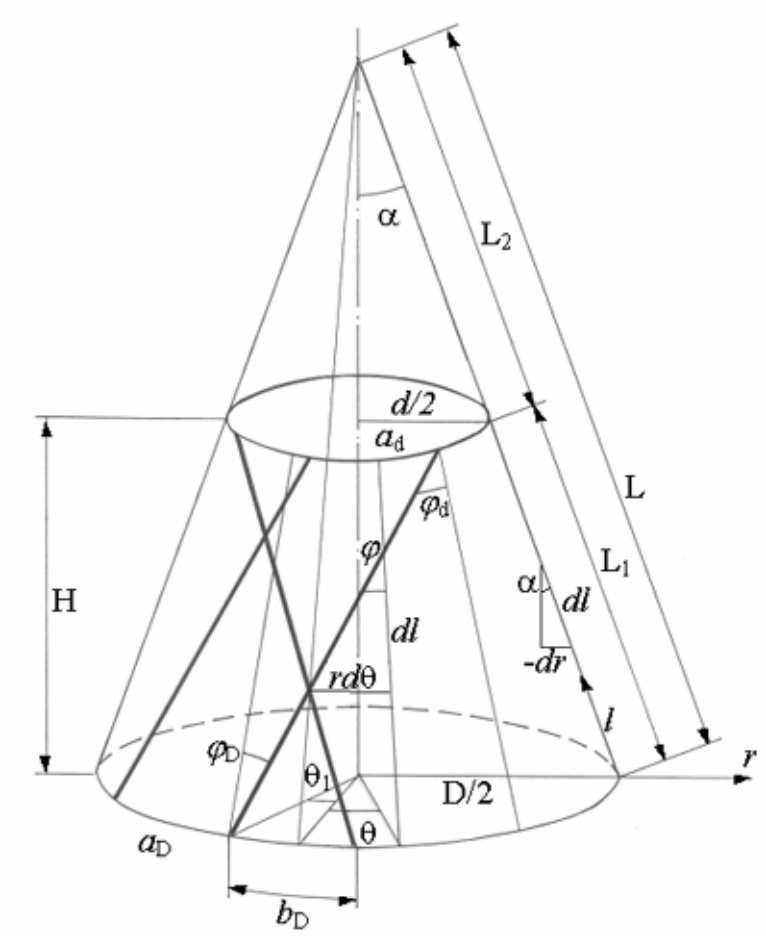

Figure 2. Geometric parameters of the structure

In accordance with Figures 1 and 2, the structure has the shape of a conical shell whose geometric parameters are linked by the following relationships

$$L = \frac{D}{2\sin\alpha}, \quad L_1 = L - L_2, \quad L_2 = \frac{d}{2\sin\alpha}, \quad H = \frac{D-d}{2}\cot\alpha \tag{1}$$

As can be seen in Figure 1, the structure consists of helical ribs and circumferential ribs located between the points of intersection of symmetric helical ribs. Such location of circumferential ribs allows us to increase the structure resistance to local buckling of helical ribs. Helical ribs are directed along geodesic lines of a conical surface, so that the rib trajectory is governed by the following equations

$$r\sin\varphi(r) = r_o$$
$$r_o = \frac{D}{2}\sin\varphi_D = \frac{d}{2}\sin\varphi_d \tag{2}$$

Here and after, subscripts "D" and "d" correspond to the variables given at $r = D/2$ and $r = d/2$, respectively. The number of helical ribs (n_h) passing trough the cone cross section r = constant is

$$n_h = 2\pi/\overline{a}_D\,, \qquad \overline{a}_D = a_D/D \tag{3}$$

in which a_D is the distance between helical ribs shown in Figure 2. The rib trajectory can be determined by integration of the following equations (see Figure 2)

$$\frac{rd\Theta}{dl} = \tan\varphi(r), \qquad \frac{dr}{dl} = -\sin\alpha \tag{4}$$

in which $\varphi(r)$ is specified by Eqn. (2).
The structure mass can be expressed as

$$M = M_r + M_h + M_c \tag{5}$$

Here, M_r is the mass of the end rings shown in Figure 1 which depends on structural parameters of the ribs, particularly, on the ribs height (the shell thickness) and the structure of joints. Using Eqns. (3) and (4), the mass of helical ribs (M_h) can presented in the following final form

$$M_h = \frac{\pi Dd}{\sin\alpha}\rho_h h\overline{\delta}_h c\left(\overline{D}c - t\right) \tag{6}$$

in which

$$\overline{\delta}_h = \delta_h/a_D^h\,, \qquad \overline{D} = D/d\,, \qquad t = \sqrt{1-\overline{D}^2 s^2}\,, \qquad c = \cos\varphi_D\,, \qquad s = \sin\varphi_D\,,$$

ρ_h is the density of helical ribs, h and δ_h are the height and the width of the helical rib cross section (which is rectangular) and a_D^h is the spacing of helical ribs counted along the normal to the rib axes at $r = D/2$, i.e., $a_D^h = ca_D$ in which a_D is shown in Figure 2. The mass of circumferential ribs (M_c) depend on the number of ribs (n_c) and their location. The radius of the first rib $(i = 1)$ and the radius of the last rib $(i = n_c)$ must satisfy the following conditions: $r_1 < D/2$, $r_{n_c} > d/2$. For circumferential ribs located between the points of intersection of symmetric helical ribs as in Figure 1, the final expression for M_c is

$$M_c = 2\pi h \rho_c h \bar{\delta}_c c\left(\bar{D}c - t\right)R_c \tag{7}$$

in which, in addition to the previous notations,

$$\bar{\delta}_c = \delta_c / a_D^c, \qquad R_c = \sum_{i=1}^{n_c} r_i,$$

ρ_c is the density of circumferential ribs, δ_c is the width of the circumferential rib cross section, a_D^c is the distance between the cross section $r = D/2$ and the first circumferential rib counted along the shell meridian and r_i is the rib radius which can be calculated as

$$r_i = \frac{r_o}{2}\left\langle \sqrt{\frac{2}{1-\cos 2\left\{\varphi_D + \sin\alpha\left[\bar{b}_D + (i-1)\bar{a}_D\right]\right\}}} + \sqrt{\frac{2}{1-\cos 2\left[\varphi_D + \sin\alpha\left(\bar{b}_D + i\bar{a}_D\right)\right]}} \right\rangle$$

in which $\bar{b}_D = b_D / D$ and b_D is shown in Figure 2.

The structure is designed for minimum mass in Eqn. (5) with respect to design variables φ_D, h, δ_h, δ_c, a_D under strength and buckling constraints.

For the structure experiencing axial compression and bending, we introduce the reduced axial force

$$P_r = P + \frac{2M}{r}$$

in which P is the axial compressive force acting on the structure and M_r is the bending moment acting in the cross section r = constant. For the end cross sections $r = D/2$ and $r = d/2$, we have, respectively

$$P_D = P + \frac{4M_D}{D}, \qquad P_d = P + \frac{4M_d}{d}$$

in which M_D and M_d are the bending moments acting at the lower and the upper sections of the adapter.

Because compressive strength of carbon-epoxy composites used to fabricate lattice adapters is lower than their tensile strength, the strength constraint must be written for the maximum compressive stress acting in helical ribs. The compressive stress in the ribs is

$$\sigma_h = \frac{P_r}{n_h h \delta_h \cos\varphi \cos\alpha} \tag{8}$$

Analysis of this equation shows that σ_h reaches its maximum value at the upper cross section of the structure $\left(r = d/2\right)$. After some transformation with the aid of Eqns. (2) and (3), we get for the maximum stress

$$\sigma_h^m = \frac{P_d}{2\pi D h \bar{\delta}_h t \cos\alpha} \tag{9}$$

So, the strength constraint can be written as $\sigma_h^m \le \bar{\sigma}$ in which $\bar{\sigma}$ is the ultimate compressive stress of the helical rib material. To formulate the global buckling constraint, we presume that

− the buckling mode is axisymmetric,

− buckling takes place in the vicinity of the shell large diameter D,

− buckling load is the same that for a lattice cylindrical shell with radius $R = D/2\cos\alpha$.
Then, using equation for the buckling load of a cylindrical lattice shell [4], we arrive at the following expression for the critical axial force

$$P_{cr} = 2\pi\sqrt{\frac{2}{3}}h^2c^2\sqrt{E_hE_c\bar{\delta}_h\bar{\delta}_c}\cos^2\alpha \tag{10}$$

in which E_h and E_c are elastic modulus of helical and circumferential ribs. Thus, the global buckling constraint acquires the form $P_D \le P_{cr}$.
To formulate the local buckling constraint, we use the Euler formular for the segment of a helical rib and write the critical stress as

$$\sigma_{cr} = k\frac{\pi^2E_h\delta_h^2}{12l_h^2} \tag{11}$$

In this equation which is valid for $h \ge \delta_h$, k is the coefficient depending on the mutual location of helical and circumferential ribs and l_n is the length of the segment of the helical rib between the points of intersection of symmetric helical ribs. For the structure in which circumferential ribs are located between these points as in Figure 1, k=4. To write the local buckling constraint, we should take into account that σ_{cr} in Eqn. (11) is minimum in the vicinity of the larger diameter D_2 where l_h is maximum, whereas the acting stress in Eqn. (8) is maximum in the vicinity of the smaller diameter d (see Figure 1). Analysis of Eqns. (8) and (11) allows us to conclude that local buckling of helical ribs takes place in the vicinity of the larger diameter D, and the critical force causing the local buckling can be presented as

$$P_{cr}^l = \frac{2}{3}k\pi^3E_hDh\bar{\delta}_h^3c^4s^2\cos\alpha \tag{12}$$

So, the local buckling constraint is $P_D \le P_{cr}^l$.
To optimize the structure, we use the Method of Minimization of Safety Factors [6] according to which strength and buckling constraints are presented in the form of the following equalities

$$n_s\sigma_h^m = \bar{\sigma}, \qquad n_oP_D = P_{cr}, \qquad n_lP_D = P_{cr}^l \tag{13}$$

in which coefficients n are some safety factors corresponding to three possible modes of failure − helical rib fracture under compression (n_s), global buckling of the shell (n_o) and local buckling of helical ribs (n_l). Note that $n \ge 1$. The case n=1 means that the corresponding constraint is active.
Using the strength constraint in Eqns. (9) and (13) and the local buckling constraint in Eqns. (12) and (13), we can express design variables $\bar{\delta}_h$ and h in terms of the corresponding safety factors as

$$\bar{\delta}_h = \frac{1}{\pi cs}\sqrt{\frac{3n_lP_D\bar{\sigma}t}{kn_sP_dE_hc}}, \qquad h = \frac{n_sP_d}{2\pi D\bar{\sigma}ct\cos\alpha}\cdot\frac{1}{\bar{\delta}_h} \tag{14}$$

Applying the global buckling constraint in Eqns. (10) and (13) and using Eqns. (14), we get

$$\bar{\delta}_c = \frac{3n_o^2 P_D^2 D\bar{\sigma}t}{4\pi m_s P_d E_h E_c c^3 \cos^3\alpha} \cdot \frac{1}{h^3} \tag{15}$$

Thus, Eqns. (14) and (15) allow us to express $\bar{\delta}_h$, h and $\bar{\delta}_c$ in terms of the safety factors and angle φ_D $(\cos\varphi_D = c)$. Substituting Eqns. (14) and (15) into Eqns. (6) and (7), we can write Eqn. (5) for the structure mass in the following form

$$M = M_r + \frac{n_s P_d d\rho_h}{\bar{\sigma}\sin 2\alpha}\left(\frac{\bar{D}c}{t} - 1\right) + \frac{18n_o^2 n_l P_D^3 D^3 \bar{\sigma}^4 t^4 \rho_c a_D^c R_c}{n_s^4 P_d^4 E_h^2 E_c s^2 c^4 \cos\alpha} \tag{16}$$

As follows from this equation, the structure mass increases with the rise of safety factors n_o and n_l.Because M must be minimum, we must take the minimum values $n_o = 1$ and $n_l = 1$. This means that both buckling constraints are active.
If we take $n_o = 1$ and $n_l = 1$ in Eqn. (16), it will include only one safety factor − n_s. Applying the minimum condition $\partial M/\partial n_s = 0$, we arrive at

$$n_s^5 = \frac{144D^2\bar{D}P_D^3\bar{\sigma}^5 t^4 \rho_c a_D^c R_c \sin\alpha}{P_d^5 k\rho_h E_h^2 E_c\left(\frac{\bar{D}c}{t} - 1\right)\sin^2\varphi_D \cos^4\varphi_D} \tag{17}$$

This equation allows us to find φ_D. To solve it, we plot the dependence $n_s(\varphi_D)$ and single out angles φ_D which correspond to n_s values that are equal or higher than unity. Substituting thus found solutions (n_s, φ_D) into Eqn. (16) (in which $n_o = n_l = 1$), we can plot dependence $M(n_s, \varphi_D)$ satisfying Eqn. (17) and condition $n_s \geq 1$. The minimum value of M provides the optimum value of φ_D and the corresponding safety factor n_s for the strength constraint.
Designed structure is analysed for all loading cases using FEM in which all segments of the ribs and the end rings are simulated with beam-type finite elements. Global buckling mode under bending is shown in Figure 3.

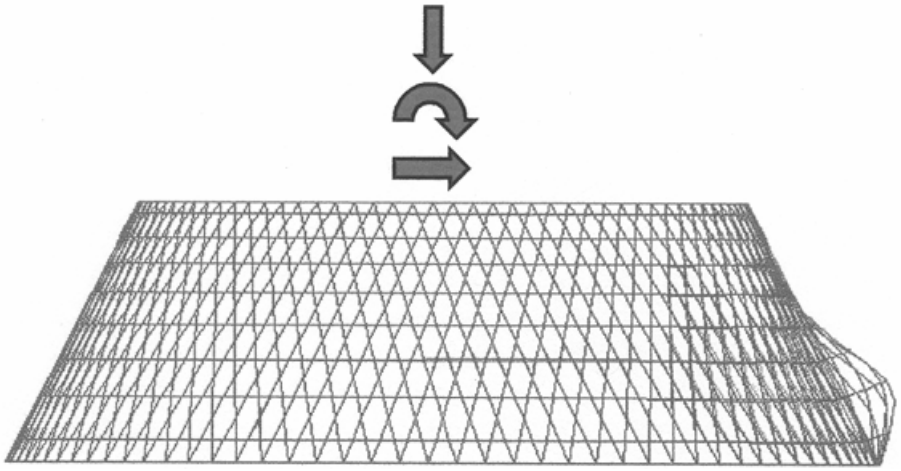

Figure 3. Finite Element simulation of the bending buckling mode

3. MANUFACTURING AND TESTING

Anisogrid lattice composite structures are manufactured by continuous wet filament winding during which carbon fiber tows impregnated with epoxy resin are placed into the grooves formed in elastic coating of the mandrel. The coating is assembled of silicon rubber panels which are fixed on the mandrel before winding and are pulled out of the lattice structure after curing. The winding process is shown in Figure 4.

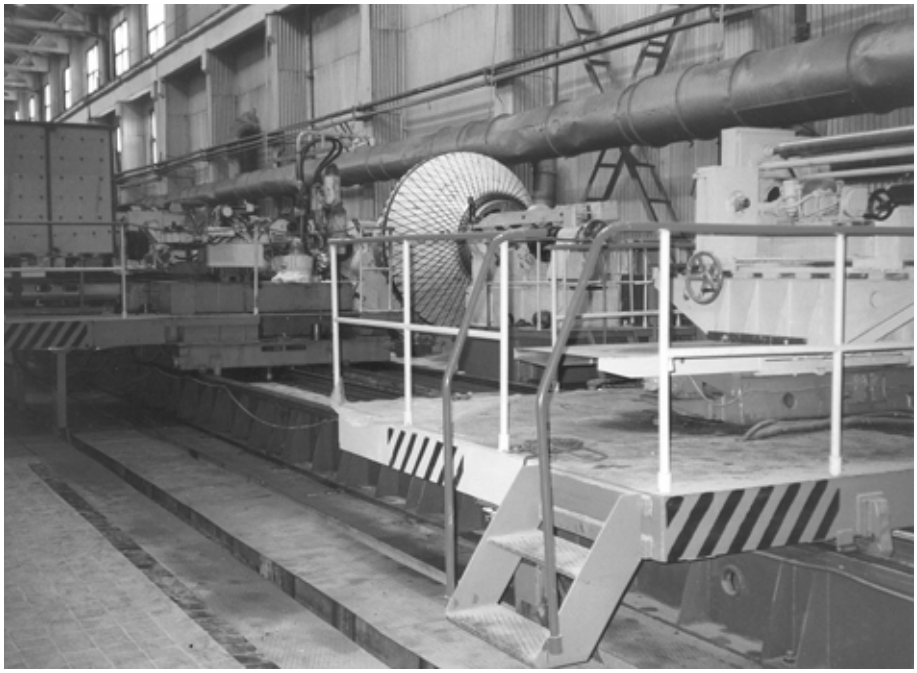

Figure 4. Winding of a lattice adapter

After winding, curing and elimination of the mandrel and the rubber panels, the structure is machined over its outer surface and the end rings surfaces (Figure 5).

Figure 5. Machining of the lattice adapter

Manufactured adapter is tested for all loading cases including static and dynamic loading. Failure modes under bending are shown in Figure 6.

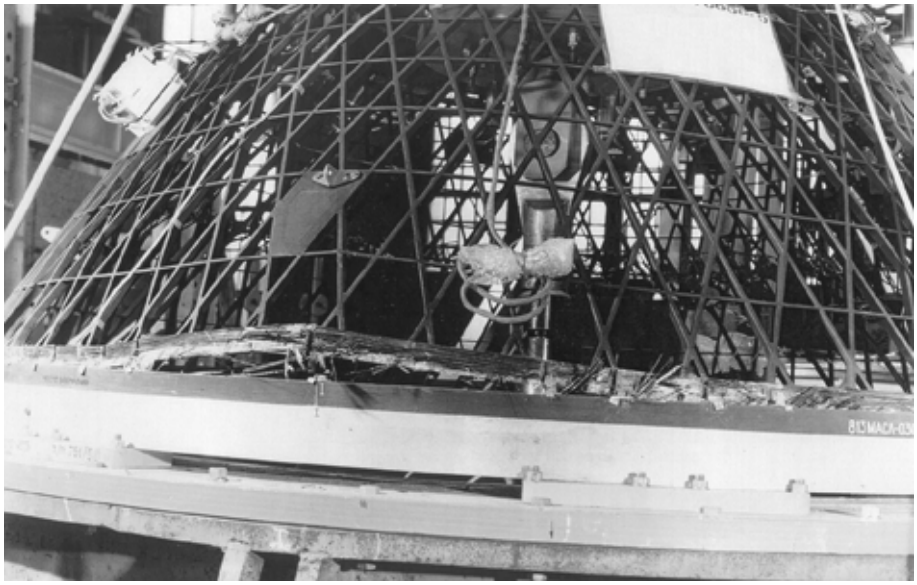

(a)

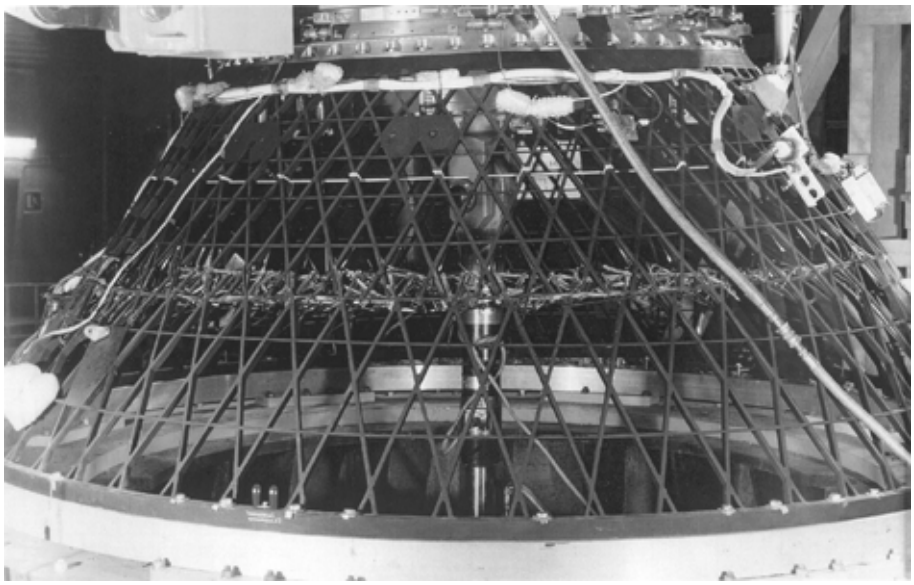

(b)

Figure 6. Failure modes in the areas of tension (a) and compression (b)

4. CONCLUSION

Composite lattice adapter which is under serial production in the Central Research Institute for Special Machinery for commercial launcher Proton-M is presented in Figure 1. The structure has the following parameters (Figure 2)

− D=2500 mm,
− d=1200 mm,
− H=1000 mm,
− M=43 kg.

Experimentally determined axial compressive force is P=1350 KN, axial stiffness is 400 KN/mm.

Two flights of Proton-M have shown high performance and very high weight efficiency of the adapter with respect to which there are no metal or composite structures developed by now for the same application which can compete anisogrid lattice structures.

References:

1. **Nosaki,Y., Takamatsu, H., Fukushima, Y.,** and **Matsubara, S.,** "Development of CFRP spacecraft attach fitting," Proc. of 13-th Int. Symp. of Space Technology and Science, Tokyo (1982), 373-378.
2. **Nakamura, T., Morino, Y., Endo, T. and Kobayashi,** M., "CFRP application to upper stage structure of Japan`s launch vehicles," Proc. of the 4-th Japan-US Conf. on Composite Materials, Washington (1988), 923-932.
3. **Hou, A. and Gramoll, K.,** "Design, damage tolerance and filament wound attach fitting for launch vehicle," *Journal of Advanced Materials*, 30/1 (1988), 16-21.
4. **Vasiliev, V.V., Barynin, V.A. and Razin, A.F.,** "Anisogrid lattice structures − survey of development and application, *Composite Structures*, 54 (2001), 361-370**.**
5. **Vasiliev, V.V., Grudzin, A.L., Petrokovskii, S.A. and Razin, A.F.,** "Lattice composite structure for the interface between the launch-rocket and the spacecraft," *Polyot*, 9 (1999), 44-46 (in Russian).
6. **Vasiliev, V.V. and Razin, A.F.,** "Optimal design of filament-wound anisogrid composite lattice structures," Proc. of the 16-th Annual Techn. Conf. of American Soc. for Composites, Blackburg (2001), (CD-ROM).